Product Release during the First Turnover of the ATP Sulfurylase−GTPase†

Sean Sukal and Thomas S. Leyh*

The Department of Biochemistry, Albert Einstein College of Medicine, 1300 Morris Park Avenue, Bronx, New York 10461-1926

Received August 30, 2001; Revised Manuscript Received October 12, 2001

ABSTRACT: ATP sulfurylase, from *Escherichia coli* K-12, is a GTPase target complex that catalyzes and couples the chemical potentials of two reactions: GTP hydrolysis and activated sulfate (APS) synthesis. Previous work suggested that the product release branch of the GTPase mechanism might include rate-determining release and/or isomerization step(s). Such steps are known to couple chemical potentials in other energy transducing systems. Rate-determining, product release step(s) were confirmed in the ATP sulfurylase−GTPase reaction by a burst of product in pre-steady-state, rapid-quench experiments. Classical rapid-quench experiments, which measure total product formation, do not allow the slow steps to be assigned to the release of a specific product, or to slow isomerization, because they do not distinguish solution-phase from enzyme-bound product. Assay systems that exclusively monitor solution-phase P_i and GDP were used to obtain free product progress curves during the first turnover of ATP sulfurylase. Together, the free and total product data describe how the products partition between the enzyme surface and solution during the first turnover. In combination, the data provide the time dependence of the concentrations of specific product intermediates, AMP·PP_i·E·GDP·P_i and AMP·PP_i·E·GDP, the rate constants for the release of P_i (4.2 s^{-1}) and GDP (4.8 s^{-1}) from these complexes, respectively, and the equilibrium constant for the enzyme-bound, β,γ-bond cleavage reaction: [AMP·PP_i·E·GTP′]/[AMP·PP_i·E·GDP·P_i] = 0.7. The data are fit, using global analysis, to obtain a complete kinetic and energetic description of this GTPase reaction.

Sulfate, a nonreactive compound, is chemically activated in metabolism by transfer of the adenylyl moiety of ATP (∼AMP) from pyrophosphate to sulfate to form activated sulfate (adenosine 5′-phosphosulfate or APS) (reaction 1). The chemical potential of the phosphoric−sulfuric acid anhydride bond formed in the transfer is remarkably large ($\Delta G^{\circ\prime}_{hydrolysis} \sim -19$ kcal/mol). Consequently, and despite cleavage of the α,β bond of ATP, APS synthesis is extremely unfavorable, $K_{eq} = 1.1 \times 10^{-8}$ [$\Delta G^{\circ\prime} = -11$ kcal/mol (*1*−*3*)]. Enzymes that labor against such equilibria to provide essential metabolites must overcome the unfavorable mass action problem, as well as the attendant kinetic problem that requires it, in this case, to "give up" 1.1×10^{-8}-fold in *V*/*K* in the forward versus the reverse direction. Thus, if the enzyme is a reasonably good catalyst in the favorable direction, it will likely be quite poor in the unfavorable direction. Nature has solved this problem, in *Escherichia coli* and other Gram-negative bacteria, by creating a GTPase target complex that couples the chemical potential of GTP hydrolysis to the synthesis of activated sulfate.

ATP sulfurylase (ATP:sulfate adenylyltranferase, EC 2.7.7.4), from *E. coli* K-12, catalyzes and conformationally couples the hydrolysis of GTP and the synthesis of activated sulfate (*4*, *5*). The enzyme is a tetramer of heterodimers (*6*). Each dimer is composed of a GTPase subunit (CysN, 53 kDa) and an APS synthesis subunit (CysD, 35 kDa) (*7*). The potential energy of these reactions are linked by changing allosteric interactions between the two active sites during the catalytic cycle that oblige the chemistries to proceed in a stepwise fashion, resulting in a well-defined, 1:1, stoichiometry (*4*). A key energy coupling step in the mechanism is an isomerization that precedes, and rate limits, GTP hydrolysis. The isomerization occurs in response to the opening of the α,β bond of ATP and can also be elicited by the binding of both AMP and PP_i. The E·AMP·PP_i complex mimics extremely well the effects of the native reaction on k_{cat} and $k_{isomerization}$ for the GTP hydrolysis reaction (*8*, *9*) and provides a simplified system for studying the GTPase.

$$ATP^{4-} + SO_4^{2-} \leftrightarrows APS^{2-} + P_2O_7^{4-} \quad (1)$$

$$GTP^{4-} + H_2O \leftrightarrows GDP^{3-} + HPO_4^{2-} + H^+ \quad (2)$$

At a saturating concentration of GTP, the rate-limiting step among first three steps of the E·AMP·PP_i-catalyzed GTP hydrolysis reaction (i.e., GTP binding, isomerization, and β,γ-bond cleavage) is the isomerization (*8*, *9*). The rate constant for this step, 14 s^{-1}, is considerably larger than k_{cat}, 1.2 s^{-1}. Hence, the mechanism must contain rate-determining steps following β,γ-bond cleavage. Such steps might include release of either or both products and/or slow isomerization-(s). Slow product release is characteristic of energy transducing systems and is often associated with the coupling of chemical potentials (*10*−*14*). It is possible, if not likely, that slow steps in the product release branch of the ATP sulfurylase mechanism will also be involved in energy coupling. The current study provides a detailed investigation of product release in the E·AMP·PP_i-catalyzed GTP hydrolysis reaction.

† Supported by National Institutes of Health Grant GM54469.

* Corresponding author. Phone: 718-430-2857. Fax: 718-430-8565. E-mail: leyh@aecom.yu.edu.

10.1021/bi015735a CCC: $20.00
Published on Web 11/09/2001

MATERIALS AND METHODS

Materials. The materials and suppliers used in this study are as follows: restriction enzymes (New England Biolabs); Pfu polymerase (Stratagene); PEI-F TLC plates (EM Science); radionucleotides (NEN Life Science Products); Q-Sepharose fast flow and Superdex 200 prep grade resins, rabbit muscle pyruvate kinase, and lactate dehydrogenase (Pharmacia); DNA primers (Oligonucleotide Synthesis Facility, Albert Einstein College of Medicine); BL21(DE3) and BL21(DE3) pLysS *E. coli*, pET-23a(+) and pET-28a(+) plasmids, His·Bind resin (Novagen); buttermilk xanthine oxidase (XO), bacterial purine nucleoside phosphorylase (PNP), porcine brain guanylate kinase, and Sephadex G-25 gel filtration resin (Sigma); 7-(diethylamino)-3-((((2-maleimidyl)ethyl)amino)carbonyl)coumarin (MDCC) (Molecular Probes); buffers, media, nucleotides, and solvents—the highest available grades (Aldrich, Sigma, or Fisher).

ATP Sulfurylase. Native *E. coli* K-12 ATP sulfurylase was expressed in *E. coli* K-12 (*9*) and purified to >95% homogeneity as described previously (*6*). The specific GTPase activity of the E·AMP·PP_i complex of ATP sulfurylase was 1.2 units/mg (*8*).

Pyruvate Kinase and Lactate Dehydrogenase. The enzymes were exchanged into 50 mM Hepes,[1] pH 8.0/KOH (the buffer used in the studies described in this paper) using size exclusion chromatography. Initial rate studies (1/*V* versus 1/[GDP] and 1/[pyruvate]) were performed to obtain kinetic constants for pyruvate kinase and lactate dehydrogenase reactions in 50 mM Hepes, pH 8.0/KOH. The optical assays for these enzymes are described elsewhere (*15*).

Cloning and Mutagenesis of the Phosphate Binding Protein (PBP). The *phoS* coding region (accession number K01992) encodes PBP and was cloned, using PCR amplification, from a wild-type *E. coli* K-12 genomic DNA library using the following primers: 5′-ATTC**CATATG**AAAGTTATGCGTACCAC-3′ and 5′-GC**GGATCC**GTTAGTACAGCGGCTTACC-3′. The *Nde*I and *Bam*HI restriction sites in the primers (bold font) were used to insert the PBP coding region into the pET-23a(+) expression plasmid. The construct appeared to be lethal in BL21(DE3) but not in strains in which T7 polymerase is either more stringently regulated [e.g., BL21(DE3)pLysS] or absent.

The PBP signal sequence was removed, and the A197C mutation needed for fluorescent labeling of the protein was inserted using overlap PCR mutagenesis (*16*). The mutagenesis primers were (the bold sequences indicate the mutations) 5′-TATGTTGAATAT**TGT**TACGCGAAGCA-3′ and 5′-TGCTTCGCGTA**ACA**ATATTCAACATA-3′. The PBP coding region was truncated to remove its signal peptide sequence by creating a new 5′-terminus for the gene using the primer 5′-CAGATC**CATATG**GAAGCAAGCCTGA-3′. The *Nde*I restriction site (bold) in this primer and the *Bam*HI site discussed above were used to clone the truncated, mutagenized insert into the pET-28a(+) plasmid. This plasmid placed a His tag at the N-terminus of the expressed protein that was used for purification. The truncated, mutant construct was not lethal in BL21(DE3) cells, indicating that the lethality may be associated with the N-terminal signal sequence.

Purification of A197C PBP. Colonies from an overnight transformation of BL21(DE3) cells were inoculated into LB media containing ampicillin (50 μg/mL) and grown at 37 °C. IPTG was added to 0.5 mM when the cultures reached an OD_{600} of 0.5−0.6. Four hours later, the cells were harvested and lysed by sonication. The preparation of the cellular extract and His-resin chromatography were performed as recommended by the manufacturer with the exception that PMSF was added to the cell extract to 1.0 mM.

The PBP that eluted from the His·Bind resin was concentrated, and the His·Bind Wash buffer was exchanged for 10 mM Tris, pH 7.6/HCl and 1.0 mM $MgCl_2$. PBP was then loaded onto a Q-Sepharose fast flow column equilibrated in the same buffer, and a 10 column volume linear gradiant of 0−50 mM NaCl in the same buffer was applied. A single protein peak resulted. NaCl was dialyzed away, and the protein was stored at −70 °C. The protein appeared >95% homogeneous by SDS−PAGE. Approximately 20 mg of pure PBP were obtained per liter of cell culture.

Labeling A197C PBP with the Fluorophore N-[2-(1-maleimidyl)ethyl]-7-(diethylamino)coumarin-3-carboxamide (MDCC). Efficient labeling of A197C PBP with MDCC requires that trace P_i in the reaction mixture be reduced substantially (*17*). This is accomplished using purine nucleoside phosphorylase (PNP), which converts P_i and inosine to hypoxanthine and ribose 1-phosphate. P_i is further reduced by the addition of phosphodeoxyribomutase (PDRM), which converts the ribose 1-phosphate to ribose 5-phosphate. PDRM is not commercially available. Our protocols replace PDRM with xanthine oxidase (XO), which is stable and commercially available. XO converts hypoxanthine to xanthine and xanthine to uric acid in what are considered irreversible reactions. The labeling protocol is as follows: PBP (100 μM), inosine (1.0 mM), $MgCl_2$ (1.0 mM), PNP (0.2 unit/mL), XO (0.2 unit/mL), MDCC (500 μM, from a 1.0 mg/mL stock in DMSO), and Hepes, 50 mM, pH 8.0/KOH. The solution was mixed overnight at 4 ± 2 °C, passed through a 0.2 μm filter to remove particulate MDCC, and loaded onto a Sephadex G-25 column equilibrated in Hepes, 50 mM, pH 8.0/KOH. The labeled protein was pooled and loaded onto a Q-Sepharose fast flow anion-exchange column equilibrated in Hepes, 50 mM, pH 8.0/KOH. The pure protein eluted off the column within 2 column volumes of this buffer; no salt was necessary. The protein was concentrated and dialyzed against the P_i-mop system and stored at −70 °C.

Quench-Flow Experiments. The experiments were performed using a KinTek quench-flow apparatus, model RQF-3. After quenching, samples were incubated in a boiling water bath for 1 min, and the radiolabeled reactants and products were separated on 10 cm PEI-F TLC sheets using 0.9 M guanidine hydrochloride as the mobile phase (*5*). The P_i and GTP were quantitated using a phosphoimager.

Fluorescence Stopped-Flow Measurements. Successful stopped-flow experiments required that P_i be scrupulously removed from the reagents and the reagent contact surfaces of the instrument. PNP using 7-methylguanosine was used to scavenge P_i (*18*). P_i was removed from the labeled PBP

[1] Abbreviations: EDTA, ethylenediamine-*N*,*N*,*N*′,*N*′-tetraacetic acid; Hepes, 4-(2-hydroxyethyl)-1-piperazineethanesulfonic acid; mant-nucleotides, 3′-*O*-(*N*-methylanthraniloyl)-2′-deoxynucleotide; PEI-F, poly(ethylenimine)−cellulose-F; PMSF, phenylmethanesulfonyl fluoride; Tris, tris(hydroxymethyl)aminomethane; unit, micromoles of substrate converted to product per minute at V_{max}.

and ATP sulfurylase by dialyzing the concentrated enzymes against buffer containing PNP (1 unit/mL), 7-methylguanosine (1.0 mM), and $MgCl_2$ (1.0 mM). Buffer was also dialyzed against the mop system by placing PNP inside the dialysis tubing. The fluorescence stopped-flow syringes and sample lines were treated for 30 min with the PNP containing buffer and then rinsed in mop-treated buffer without PNP. PNP was kept at a very low level (0.04 unit/mL) in both syringes. This reduced P_i prior to starting the experiment and was sufficiently low that PNP did not compete with PBP for P_i.

An Applied Photophysics SX-18MV stopped-flow spectrometer was used for these experiments. The samples were equilibrated, and the time courses were measured at 25 ± 2 °C. For the PBP-MDCC experiments, the excitation wavelength was 425 nm; light emitted above 455 nm was detected using a cutoff filter. The GDP release and guanylate kinase experiments detected the NADH emission above 400 nm, exciting at 340 nm. In all cases, five to eight scans were averaged. Where possible, the concentration of the nonfluorescent rather that fluorescent species was varied. This strategy improves data quality and simplifies the experimental protocols by allowing the data to be gathered at one instrument setting.

RESULTS AND DISCUSSION

A Burst of Product. Rapid-quench experiments were performed to test for the presence of slow steps in the product release portion of the GTPase reaction. The E·AMP·PP_i complex was mixed rapidly with a saturating concentration of GTP and allowed to react for a defined period before being mixed rapidly with a quench solution (see Materials and Methods). The results reveal a pre-steady-state burst of product, followed by linear steady-state turnover of the enzyme (see Figure 1). To ensure that the burst was linear with enzyme concentration, each time point was performed, in triplicate, at two concentrations of enzyme [20 μM (●) and 100 μM (○)]. The signal-to-noise ratio was better in the 100 μM experiments, particularly at the early time points, and these data were used in all subsequent quantitative analyses. The burst amplitude was 0.32 of an enzyme active site, and k_{cat}, 1.22 ± 0.04 s^{-1}, was in good agreement with control steady-state measurements performed at catalytic concentrations of ATP sulfurylase (k_{cat} = 1.2 s^{-1}).

The burst of product confirms that product release and/or an isomerization in the release stage of the reaction is at least partially rate-limiting turnover. A burst of <1 enzyme active site equivalent occurs when the rate of product formation is comparable to that for product release and/or from an internal equilibrium constant that is not largely in favor of product (*19*). As will be shown, both of these factors contribute to the observed burst amplitude. ATP sulfurylase is competent to bind 1 active site equivalent of GTP (*20*), and single-turnover experiments show that the hydrolysis of mant-GTP, a fluorescent analogue of GTP, is monophasic and that all of the nucleotide is hydrolyzed (*21*). Thus, partially active enzyme or fraction-of-the-sites reactivity are unlikely explanations for the substoichiometric burst.

Classical rapid-quench experiments can be useful in assessing whether product release is rate limiting; however, in systems involving more than one product, they do not provide the information needed to assign the slow steps to specific events in the product release section of the catalytic cycle. The reason the steps cannot be assigned is that the experiments do not distinguish between enzyme-bound and solution-phase product; they report, instead, on the sum of all of the product forms. A burst in total product predicts a complementary lag in the formation of solution-phase product. If the delivery of each product into solution could be monitored during the first turnover, it would be possible, in favorable cases, to assign the order of product release, to obtain rate constants for release steps, and to identify slow isomerization steps that follow product release. Together, the progress curves for total and free product provide a complete description of the partitioning of product between the enzyme and solution during the first turnover of the reaction.

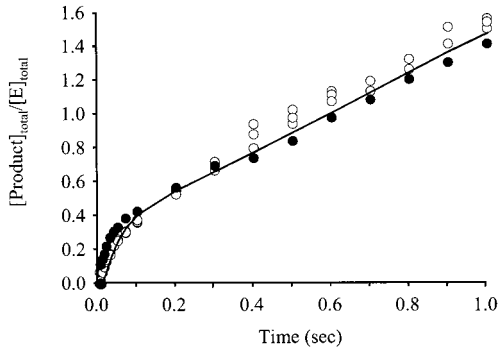

FIGURE 1: GDP/P_i formation during the first turnover of ATP sulfurylase. A solution containing ATP sulfurylase [40 μM (●) or 200 μM (○)], AMP (1.0 mM), PP_i (100 μM), $MgCl_2$ (2.6 mM), and Hepes (50 mM, pH 8.0/KOH) was mixed rapidly using a quench-flow apparatus with an equal volume of an identical solution that did not contain enzyme but did contain GTP/[γ-^{32}P]GTP (1.0 mM; SA = 80 μCi/mL). The mixture was aged for a defined period and quenched by rapid mixing with a basic solution of EDTA/NaOH (100 mM, pH 11.0) (*8*). The instrument and reagents were equilibrated at 25 ± 2 °C prior to mixing. Radiolabeled reactants were separated using TLC and quantitated (see Materials and Methods). Product formation was determined in triplicate at each time point. The average is shown for the lower concentration experiment (●). The smooth curve passing through the data represents the best fit of the data at 100 μM ATP sulfurylase to an ordered release model (see The Global Fit).

The Free GDP Assay. Solution-phase GDP can be quantitatively consumed and stoichiometrically (1:1) linked to the oxidation of free NADH using the pyruvate kinase−lactate dehydrogenase (PK-LDH) coupled assay system (*8*, *22*, *23*). The NADH to NAD^+ conversion can be followed by an optical density change at 340 nm or by a fluorescence change above 400 nm, exciting at 340 nm. Like all coupled assay systems, the PK-LDH system exhibits a lag in product formation caused by the time required for its reactions to reach the steady state. It is critical that this intrinsic lag be short compared to the lag associated with the release of GDP during the first turnover of ATP sulfurylase. Previous analyses of coupled enzyme assays (*24*−*27*), and computer simulations, were used to estimate the coupling enzyme concentrations needed to attain the desired lag time.

Guanylate kinase, which converts GMP and GTP to two GDP (*28*), was used at catalytic concentrations to assess the intrinsic lag under conditions that matched the steady-state velocity of guanylate kinase-catalyzed GDP synthesis to that of the pre-steady-state ATP sulfurylase experiments. This allows the behavior of the coupling system to be evaluated

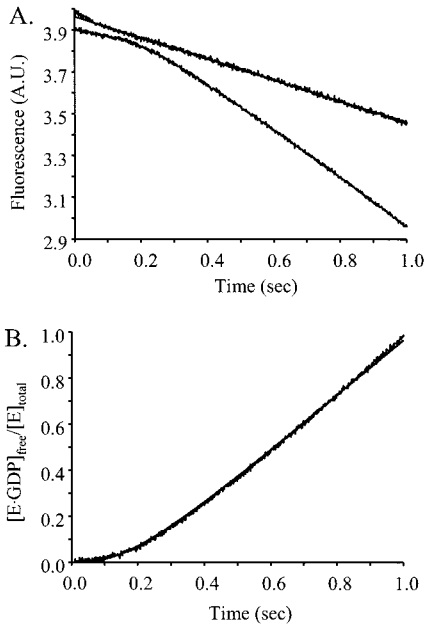

FIGURE 2: GDP release during the first turnover of the E·AMP·PP_i complex of ATP sulfurylase. Panel A: Response time of the GDP sensor. The upper curve was generated by mixing a solution containing guanylate kinase (2.5 units/mL of GDP forming activity from GTP and GMP), $MgCl_2$ (3.2 mM), and Hepes (50 mM, pH 8.0/KOH) with an equal volume of a solution containing pyruvate kinase (200 μM), lactate dehydrogenase (72 μM), NADH (284 μM), PEP (2.0 mM), GTP (2.0 mM), GMP (2.0 mM), $MgCl_2$ (3.2 mM), and Hepes (50 mM, pH 8.0/KOH) in the fluorescence stopped-flow apparatus. The reaction was monitored using the change in fluorescence intensity that NADH undergoes as it is converted to NAD^+. The lower trace is the time course generated by mixing a solution containing ATP sulfurylase (40 μM), AMP (1.0 mM), PP_i (100 μM), $MgCl_2$ (2.7 mM), and Hepes (50 mM, pH 8.0/KOH) with a solution containing pyruvate kinase (200 μM), lactate dehydrogenase (72 μM), NADH (284 μM), PEP (2.0 mM), GTP (1.0 mM), AMP (1.0 mM), PP_i (100 μM), $MgCl_2$ (2.7 mM), and Hepes (50 mM, pH 8.0/KOH), $T = 25 \pm 2$ °C. Panel B: Solution-phase GDP formation during the first turnover of ATP sulfurylase. The release of GDP was monitored by the fluorescence change of NADH upon conversion to NAD^+ by the PK-LDH coupled enzyme assay. The conditions for this experiment were the same as for the ATP sulfurylase experiment described in panel A. Fluorescence was converted to GDP concentration using a standard curve (see text).

under conditions essentially identical to those of the ATP sulfurylase experiment but without a detectable burst or lag. The results are shown in Figure 2, panel A. The guanylate kinase time course is very nearly linear back to $t = 0$, while the time course obtained using the E·AMP·PP_i complex of ATP sulfurylase exhibits a pronounced lag. The coupling enzyme concentrations chosen for this experiment (see Figure 2 legend) were used in subsequent experiments to evaluate the release of GDP from ATP sulfurylase.

GDP Release during the First Turnover. The release of GDP during the first turnover of the E·AMP·PP_i complex of ATP sulfurylase is shown in Figure 2, panel B. In this experiment, a solution containing ATP sulfurylase (40 μM) and a saturating concentration of AMP (1.0 mM) and PP_i (100 μM) was mixed rapidly, using a stopped-flow fluorometer, with a solution containing a saturating concentration of GTP and the PK-LDH coupling system (see Materials and Methods and the Figure 2 legend). The change in fluorescence intensity was converted to GDP concentration using a standard curve calibrated by conducting stopped-flow experiments identical to those associated with Figure 2 except that ATP sulfurylase, AMP, and PP_i were replaced by GDP, at a known concentration. The ~170 ms lag in the appearance of GDP in solution demonstrates that it is released slowly by the E·AMP·PP_i complex and that this step either is or precedes a rate-determining event in the product release phase of the reaction. k_{cat} obtained from the steady-state region of the time course is equivalent to that obtained from the total product time course, 1.2 s^{-1}.

Phosphate Binding Protein (PBP), the Free P_i Assay. The phosphate binding protein system was used to assay solution-phase phosphate. This system used the phosphate binding protein, from *E. coli* K-12, that is covalently labeled with a fluorophore, MDCC, at cysteine-197, which is located near the P_i binding pocket (*18*, *29*−*31*). Upon binding of P_i, the PBP-bound MDCC undergoes a 13-fold increase in fluorescence intensity (*17*). To acquire this system for these studies, the structural gene for the phosphate binding protein, *phoS*, was cloned from a genomic *E. coli* K12 library. The *phoS* leader peptide, which caused lethality, was removed, and the A197C mutation was inserted (see Materials and Methods). An N-terminal, His-tag expression system was constructed, and the protein was purified and labeled at C197 with MDCC (see Materials and Methods).

Stopped-flow fluorescence experiments were used to assess the P_i binding characteristics of the system. The binding of P_i to PBP was studied under pseudo-first-order conditions with respect to P_i concentration. The reactions were monophasic, and their associated k_{obs} values were plotted versus P_i concentration (Figure 3, panel A). The resulting, linear plot was fit to eq 3 to obtain k_{on} and k_{off}, 1.5×10^8 M^{-1} s^{-1} and

$$k_{obs} = k_{on}[P_i] + k_{off} \quad (3)$$

29 s^{-1}, respectively. These rate constants predict a K_d of 0.19 μM and are quite similar to those for the non-His-tagged PBP (*18*). The binding of P_i to PBP is extremely fast and favorable, and any lag associated with the binding reaction is within the limit of resolution of the instrument, ≤3 ms.

P_i Release during the First Turnover. The release of P_i from the E·AMP·PP_i complex of ATP sulfurylase during the first turnover of the enzyme was monitored using stopped-flow fluorescence (Figure 3, panel B). The experimental design was identical to that described for GDP release, except that the PBP assay system replaced the PK-LDH system, and the optics were changed (see Materials and Methods). The fluorescence changes were converted to P_i concentration by calibration using stopped-flow experiments that mixed the PBP assay solution described in the Figure 3 legend with solutions of known P_i concentration. The lag associated with the release of P_i is short, 30 ms, but well within the resolution of the instrument and the PBP assay system. Thus, during the burst phase, P_i departs more quickly than GDP from the active site, indicating that P_i release occurs before, or is concomitant with, the release of GDP.

Data Analysis. The progress curves for total and solution-phase product can be combined to describe the time dependence of the formation of specific enzyme-bound intermediates in the catalytic cycle. Interpretation of the combined data depends on the product complexes of the mechanism used for the analysis. The affinity of GDP, or mant-GDP, for the ground-state complexes of ATP sulfur-

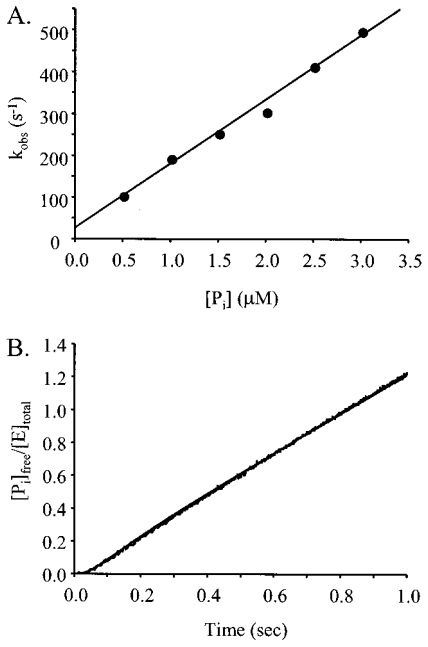

FIGURE 3: Phosphate release during the first turnover of the E·AMP·PP_i complex of ATP sulfurylase. Panel A: Phosphate binding to the fluorescent phosphate binding protein (PBP-MDCC). A solution containing P_i at two times the indicated concentration was mixed with an equal volume of a solution containing PBP-MDCC (0.30 μM) in the fluorescence stopped-flow apparatus, $T = 25 \pm 2$ °C. The buffer, Hepes (50 mM, pH 8.0/KOH), was treated with the P_i-mop system to reduce background levels of P_i (see Materials and Methods). The reaction was monitored by a change in fluorescence intensity that occurs upon binding. A total of 5−8 transients were collected at each [P_i]. The averaged data were fit to a single exponential to obtain k_{obs}. The plot of k_{obs} versus [P_i] was fit to a linear equation to obtain k_{on} (1.5×10^8 M^{-1} s^{-1}), k_{off} (29 s^{-1}), and K_d (0.19 μM). Panel B: Solution-phase P_i formation during the first turnover of ATP sulfurylase. The release of P_i from ATP sulfurylase was monitored by the fluorescence change associated with the binding of P_i to PBP-MDCC. A solution containing ATP sulfurylase (40 μM), AMP (1.0 mM), PP_i (100 μM), PNP (0.04 unit/mL), 7-methylguanosine (1.0 mM), $MgCl_2$ (2.9 mM), and Hepes (50 mM, pH 8.0/KOH) was mixed with an equal volume of a solution containing PBP-MDCC (100 μM), PNP (0.04 unit/mL), 7-methylguanosine (1.0 mM), and Hepes (50 mM, pH 8.0/KOH), $T = 25 \pm 2$ °C. Fluorescence was converted to P_i concentration using P_i standards (see text).

ylase varies between 10 and 40 μM (*21*, *32*), while the affinity of P_i is so low that it is difficult to measure (*32*); however, K_m for the binding of P_i to the E·APS·PP_i·GDP complex has been determined, 44 (±14) mM (*33*). These facts suggest that the release of GDP and P_i from ATP sulfurylase is either ordered, with P_i departing prior to GDP, or random, with a highly preferred release sequence in which P_i departs first. Thus, under initial rate conditions, where the concentration of P_i is low, the ordered mechanism is either an exact description or an excellent approximation of the release of product in this system.

The progress curves for the enzyme-bound product intermediates are obtained by subtraction of those for solution-phase and total product. For an ordered mechanism, total product (P_t) can be written in terms of either P_i or GDP (eqs 4 and 5). Subtraction of [P_i] from [P_t] gives

$$[P_t] = [E{\cdot}GDP{\cdot}P_i] + [P_i] \quad (4)$$

$$[P_t] = [E{\cdot}GDP{\cdot}P_i] + [E{\cdot}GDP] + [GDP] \quad (5)$$

[E·GDP·P_i]], and subtraction of eq 2 from eq 1 and simple rearrangement gives [E·GDP] = [P_i] − [GDP].

The time dependence of the concentrations of E·GDP·P_i and E·GDP, normalized to total enzyme concentration, is shown in Figure 4. The concentrations of these species rise at different rates during the burst phase of the first turnover to a steady state in which 35% of the enzyme is in the E·GDP·P_i complex and 25% is in the E·P_i complex. Once *both* of the intermediates have reached steady state, the rates at which GDP and P_i are delivered to solution are identical and, under the conditions of these experiments (i.e., saturating GTP), equal to k_{cat}, 1.2 s^{-1}. Given the rates for the formation of solution-phase GDP and P_i, and the concentrations of the enzyme-bound complexes that deliver them into solution, the rate constants governing their release can be calculated using the following simple relationships: $k_{off(P_i)} = k_{cat}/([E{\cdot}GDP{\cdot}P_i]/[E_{tot}]) = 1.2\ s^{-1}/0.35 = 3.4\ s^{-1}$ and $k_{off(GDP)} = k_{cat}/([E{\cdot}GDP]/[E_{tot}]) = 1.2\ s^{-1}/0.25 = 4.8\ s^{-1}$.

During steady-state turnover, ∼60% of the enzyme is in product complexes; the remainder is distributed over the two substrate complexes, ES and ES′, and free enzyme (E) which is negligible at saturating GTP. The binding, isomerization, and bond cleavage reactions are fast in the forward direction compared to product release, and isomerization is extremely favorable, $K_{iso} = 2980$ (*21*). Thus, the majority of the ∼40% of the substrate-bound enzyme will reside in the E·GTP′ complex, which suggests that the enzyme-bound equilibrium constant for the chemical step will be near unity (i.e., [E·GTP]/ [E·GDP·P_i] ∼ 1 ∼ 0.40/0.35). This equilibrium constant can be estimated using net rate constant theory (*34*).

Under initial rate conditions, the ATP sulfurylase mechanism can be represented by eq 6 (where E = E·AMP·PP_i). The double- and single-headed arrows indicate reversible and irreversible steps of the mechanism, respectively. The product release steps, k_7 and k_9, are treated as irreversible because their reverse reaction rates are ∼0 during the initial rate phase of the reaction (*34*). Equation 6 is simplified by the theory to eq 7, where a prime indicates a net rate constant (i.e., the rate constant that would produce the same flux through the step if it were irreversible). The ratios of the concentrations

$$E + GTP \underset{k_2}{\overset{k_1}{\leftrightarrow}} E{\cdot}GTP \underset{k_4}{\overset{k_3}{\leftrightarrow}} E{\cdot}GTP' \underset{k_6}{\overset{k_5}{\leftrightarrow}} E{\cdot}GDP{\cdot}P_i \xrightarrow{k_7} E{\cdot}GDP + P_i \xrightarrow{k_9} E + GDP + P_i \quad (6)$$

$$E + GTP \xrightarrow{k_1'} E{\cdot}GTP \xrightarrow{k_3'} E{\cdot}GTP' \xrightarrow{k_5'} E{\cdot}GDP{\cdot}P_i \xrightarrow{k_7} E{\cdot}GDP + P_i \xrightarrow{k_9} E + GDP + P_i \quad (7)$$

of enzyme complexes can be calculated as follows using net rate constants and the mass ratio information described above:

$$0.40/0.35 = 1.1 = ([E{\cdot}GTP] + [E{\cdot}GTP'])/[E{\cdot}GDP{\cdot}P_i] = k_7(1/k_3' + 1/k_5') \quad (8)$$

Expressing k_3' and k_5' in terms of the mechanism's actual rate constants and rearranging:

$$1.1 = [(k_3 + k_4)k_6 + (k_3 + k_4 + k_5)k_7]/k_3k_5 \quad (9)$$

Only k_5 and k_6 are unknown. Isomerization is sufficiently

Table 1: Kinetic and Thermodynamic Constants Governing GTP Hydrolysis

reaction	$k_{forward}$	$\Delta G^{\ddagger}$ (kcal/mol)	$k_{reverse}$	$\Delta G^{\ddagger}$ (kcal/mol)
E[a] + GTP ↔ E·GTP	2.9 (±0.2) × 10^5 M^{-1} s^{-1} [b]	10.0	7.9 (±0.9) s^{-1} [b]	16.2
E·GTP ↔ E·GTP′	26 (±0.2) s^{-1}	15.5	4.7 × 10^{-3} (±0.6 × 10^{-3}) s^{-1} [b]	21.5
E·GTP′ ↔ E·GDP·P_i	160 (±2) s^{-1}	14.4	220 (±4) s^{-1}	14.2
E·GDP·P_i ↔ E·GDP + P_i	4.2 (±0.01) s^{-1}	16.5	0.0043 M^{-1} s^{-1} [c]	20.6
E·GDP ↔ E + GDP	4.8 (±0.04) s^{-1}	16.5	2.1 (±0.2) × 10^6 M^{-1} s^{-1}	8.8

[a] E represents the E·AMP·PP_i complex of ATP sulfurylase. [b] Determined previously (*9*). [c] See text for an error estimate.

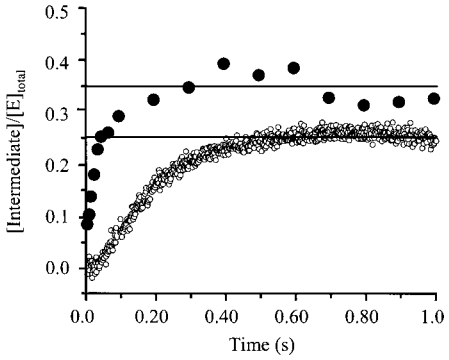

FIGURE 4: Time dependence of the concentrations of the AMP·PP_i·E·GDP·P_i and AMP·PP_i·E·GDP intermediates during the first turnover of ATP sulfurylase. The progress curves were calculated from those for total and solution-phase product (see Data Analysis). The closed circles (●) represent the AMP·PP_i·E·GDP·P_i complex; the open circles (○) represent the AMP·PP_i·E·GDP intermediate.

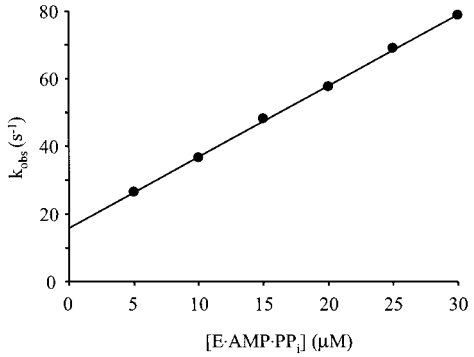

FIGURE 5: Enzyme concentration dependence of the observed rate constant for mant-GDP binding to the E·AMP·PP_i complex of ATP sulfurylase. A solution containing ATP sulfurylase at two times the indicated concentration, AMP (1.0 mM), PP_i (100 μM), $MgCl_2$ (2.1 mM), and Hepes (50 mM, pH 8.0/KOH) was mixed with an equal volume of an identical solution that did not contain enzyme but did contain mant-GDP (500 mM). The solutions were equilibrated, and the experiment was performed at 25 ± 2 °C. The binding reaction was monitored by following the change in fluorescence of the nucleotide as it binds to the enzyme. The transients were fit to a single exponential, and the resulting observed rate constants were plotted versus enzyme concentration.

fast compared to β,γ-bond breaking that these steps of the mechanism appear to be simultaneous (*21*). Thus, the rate constant for the bond cleavage step, k_5, can be estimated at ≥6 times that for the isomerization (i.e., $k_5 \geq 84$ s^{-1}). Setting $k_5 = 84$ s^{-1}, one can calculate that $k_6 = 68$ s^{-1}. The equilibrium constant for the β,γ-bond cleavage step predicted by these constants is near unity: [E·GDP·P_i]/[E·GTP′] = $k_5/k_6 = 1.2$.

The Gobal Fit. The total and free product progress curves were simultaneously fit using the global fitting program Gepasi (3.21) (*35*−*37*). During the first fitting iterations, the four rate constants governing GTP binding and isomerization, obtained from previous studies using mant-nucleotides (*9*), were held fixed, and GDP and P_i release were modeled as irreversible steps because the system is under initial rate turnover. To optimize fitting of the burst, the forward isomerization rate constant was subsequently allowed to vary, resulting in an increase from 14 s^{-1} (*9*) to 26 s^{-1}. Ordered and random product release models were tested. The ordered mechanism gave a significantly better fit; the random mechanism predicted rate constants for the alternative release path (i.e., GDP release first) that were quite small compared to those for the preferred path (0.1 and 0.4 s^{-1} for GDP and P_i release, respectively) and had very high errors (300−400%). This finding underscores that the ordered mechanism is a suitable model for the ATP sulfurylase−GTPase reaction. Previous experiments suggested that a reasonable lower limit for the β,γ-bond-breaking rate constant, k_5, was ∼6 times that of the forward isomerization step; the ratio provided by the fit is 6.2. Lowering this ratio deteriorates the quality of the fit; however, k_5 can be raised indefinitely above this lower limit without affecting the fit quality, as long as the equilibrium constant for the bond-breaking step is held fixed at 0.7. Thus, the fit provides a lower limit for the bond opening and closing rate constants. The progress curves predicted by the best-fit constants are shown as solid lines passing through the data (Figures 1−3). The best-fit constants obtained from the fit, along with their thermodynamic constants, are complied in Table 1 and agree well with those obtained from the analysis described above.

Completing the Kinetic Scheme. The two rate constants needed to complete the kinetic description of the GTPase reaction are those for the addition of GDP to the AMP·PP_i·E complex and for the addition of P_i to the AMP·PP_i·E·GDP complex. A good approximation of the constants for the addition of GDP was obtained from classical stopped-flow studies of the binding of mant-GDP to E·AMP·PP_i·E. The mant-GDP binding reactions were monophasic (data not shown). The k_{obs} vs [E·AMP·PP_i·E] plot was linear (see Figure 5), and the best fit of the data gave the following: $k_{on} = 2.1 \times 10^6$ M^{-1} s^{-1}, $k_{off} = 16$ s^{-1}, and $K_d = 7.6$ μM. The 3.3-fold difference in the release rate constants for GDP and mant-GDP suggests similar differences could be associated with the on-rate constants.

The rate constant for the association of P_i with AMP·PP_i·E·GDP can be calculated by setting the product of all of the forward rate constants, divided by that for the reverse rate constants, equal to the equilibrium constant for the overall reaction (i.e., GTP hydrolysis) and solving for the single, unknown constant, $k_{on(P_i)}$. The result of the calculation reveals that the P_i on-rate constant is extraordinarily slow, 0.0043 M^{-1} s^{-1}, and that the release of P_i is extremely favorable, $K_d = 976$ M and $\Delta G^{\circ\prime} = -4.1$ kcal/mol. The accuracy of this on-rate constant no doubt suffers both from the propagation of errors associated with the calculation and from the

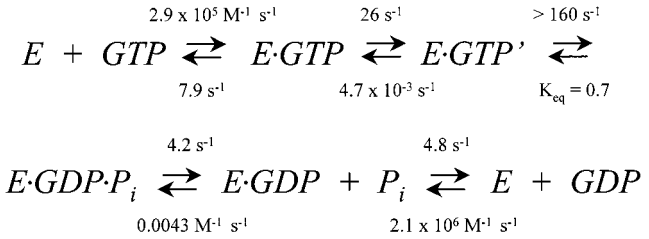

FIGURE 6: Mechanism of the E·AMP·PP_i-catalyzed hydrolysis of GTP. The rate constants were determined in the current study except for the constants governing the association of enzyme with GTP and GDP, the reverse isomerization, and GTP release, which were determined in previous work using mant-nucleotides (*9*). The prime indicates isomerization. The rate constant governing β,γ-bond cleavage is a lower limit (see text).

assumption, in certain cases, that rate constants governing the mant-nucleotide and native nucleotide behavior are equal. Nevertheless, the experimental errors are small (see Table 1), and the behavior of mant-nucleotide and native nucleotide is quite comparable. If the errors were as large as a factor of 10, the basic disposition of the P_i association step would not change; release would still be extremely favorable and the on-rate constant extremely slow. Thermodynamic constants for the addition of P_i to the E·NDP complexes of systems that hydrolyze nucleotides are difficult to measure due to the very low affinity of P_i. In cases where they have been measured, they range from ~20 to >200 mM (*33*, *38*, *39*). For most energy coupling systems that hydrolyze nucleotides, these important constants are, at present, unknown.

Mechanism and Behavior of ATP Sulfurylase. The kinetic scheme for the E·AMP·PP_i-catalyzed hydrolysis of GTP, and its rate constants, is shown in Figure 6. At 1.0 mM GTP, which is near its presumed physiological concentration (*33*), GTP binding is fast compared to turnover. The isomerization is partially rate limiting in the forward reaction, while its reverse is sufficiently slow that the system becomes irreversibly committed to completing the catalytic cycle once the isomerization has occurred. β,γ-bond cleavage is rate limited by the isomerization, and the bond-breaking and -forming steps are essentially isoenergetic. To achieve this condition, the enzyme must exhibit a profound, selective stabilization of GTP over GDP·P_i, compared to solution, that is caused by changes in enzyme−substrate interactions in the vicinity of the β,γ bond. The rate constants for release of P_i and GDP from the E·GDP·P_i and E·GDP·P_i complexes, respectively, are the slowest steps in the mechanism, and P_i release acts both as a kinetic barrier to prevent reversal of the reaction and as a thermodynamic sink to draw the system through its catalytic cycle.

CONCLUSIONS

Determining how product partitions between the enzyme active site and solution during the first turnover of ATP sulfurylase has proven a valuable method for characterizing the events that occur in the latter stages of this GTPase reaction. It provides the time dependence of the concentration of each of the product intermediates in the catalytic cycle, the order in which products are released, and the microscopic rate constants for product dissociation from these intermediates. It is also capable of detecting a rate-determining isomerization, if it occurs after product is released. The method, as described here, can be extended to other ATPase/GTPase systems and is generally applicable to other systems for which appropriate coupled assays exist.

The E·AMP·PP_i-catalyzed GTPase mechanism includes an isomerization that "toggles" the GTPase reaction, a bond-breaking step whose equilibrium constant is near unity, a remarkably unfavorable P_i binding reaction, and two partially rate-limiting product release steps. Slow product release is a characteristic of conformationally coupled systems that hydrolyze nucleotides and is often thought to be a critical energy-linking step (*10*−*14*). Given this precedent, it is plausible, if not likely, that this will also be the case in the native reaction catalyzed by ATP sulfurylase. This hypothesis will be tested by determining whether events in the APS-forming reaction are concomitant with the product release steps of the GTPase reaction.

REFERENCES

1. Robbins, P., and Lipmann, F. (1956) *J. Am. Chem. Soc. 78*, 6409−6410.
2. Robbins, P. W., and Lipmann, F. (1958) *J. Biol. Chem. 233*, 686−690.
3. Leyh, T. S. (1993) *Crit. Rev. Biochem. Mol. Biol. 28*, 515−542.
4. Liu, C., Suo, Y., and Leyh, T. S. (1994) *Biochemistry 33*, 7309−7314.
5. Leyh, T. S., and Suo, Y. (1992) *J. Biol. Chem. 267*, 542−545.
6. Leyh, T. S., Taylor, J. C., and Markham, G. D. (1988) *J. Biol. Chem. 263*, 2409−2416.
7. Leyh, T. S., Vogt, T. F., and Suo, Y. (1992) *J. Biol. Chem. 267*, 10405−10410.
8. Wang, R., Liu, C., and Leyh, T. S. (1995) *Biochemistry 34*, 490−495.
9. Wei, J., and Leyh, T. S. (1998) *Biochemistry 37*, 17163−17169.
10. Jencks, W. P. (1989) *Methods Enzymol. 171*, 145−164.
11. Hackney, D. D. (1996) *Annu. Rev. Physiol. 58*, 731−750.
12. Sleep, J. A., Hackney, D. D., and Boyer, P. D. (1980) *J. Biol. Chem. 255*, 4094−4099.
13. Johnson, K. A. (1985) *Annu. Rev. Biophys. Biophys. Chem. 14*, 161−188.
14. Gilbert, S. P., and Johnson, K. A. (1994) *Biochemistry 33*, 1951−1960.
15. Davidson, E. A. (1959) *Biochim. Biophys. Acta 33*, 238−240.
16. Innis, M. A. (1990) *PCR Protocols: A Guide to Methods and Applications*, Academic Press, San Diego.
17. Brune, M., Hunter, J. L., Howell, S. A., Martin, S. R., Hazlett, T. L., Corrie, J. E., and Webb, M. R. (1998) *Biochemistry 37*, 10370−10380.
18. Brune, M., Hunter, J. L., Corrie, J. E., and Webb, M. R. (1994) *Biochemistry 33*, 8262−8271.
19. Johnson, K. A. (1992) in *The Enzymes* (Purich, D., Ed.) Vol. XX, pp 1−61, Academic Press, New York.
20. Yang, M., and Leyh, T. S. (1997) *Biochemistry 36*, 3270−3277.
21. Wei, J., and Leyh, T. S. (1999) *Biochemistry 38*, 6311−6316.
22. Jenkins, W. T. (1991) *Anal. Biochem. 194*, 136−139.
23. Plowman, K. M., and Krall, A. R. (1965) *Biochemistry 4*, 2809−2814.
24. McClure, W. R. (1969) *Biochemistry 8*, 2782−2786.
25. Rudolph, F. B., Baugher, B. W., and Beissner, R. S. (1979) *Methods Enzymol. 63*, 22−42.
26. Cleland, W. W. (1979) *Anal. Biochem. 99*, 142−145.
27. Easterby, J. S. (1973) *Biochim. Biophys. Acta 293*, 552−558.
28. Agarwal, K. C., Miech, R. P., and Parks, R. E., Jr. (1978) *Methods Enzymol. 51*, 483−490.
29. Lionne, C., Brune, M., Webb, M. R., Travers, F., and Barman, T. (1995) *FEBS Lett. 364*, 59−62.

30. Nixon, A. E., Brune, M., Lowe, P. N., and Webb, M. R. (1995) *Biochemistry 34*, 15592−15598.
31. Gilbert, S. P., Webb, M. R., Brune, M., and Johnson, K. A. (1995) *Nature 373*, 671−676.
32. Liu, C., Martin, E., and Leyh, T. S. (1994) *Biochemistry 33*, 2042−2047.
33. Liu, C., Wang, R., Varlamova, O., and Leyh, T. S. (1998) *Biochemistry 37*, 3886−3892.
34. Cleland, W. W. (1975) *Biochemistry 14*, 3220−3224.
35. Mendes, P., and Kell, D. (1998) *Bioinformatics 14*, 869−883.
36. Mendes, P. (1997) *Trends Biochem. Sci. 22*, 361−363.
37. Mendes, P. (1993) *Comput. Appl. Biosci. 9*, 563−571.
38. Amory, A., Goffeau, A., McIntosh, D. B., and Boyer, P. D. (1982) *J. Biol. Chem. 257*, 12509−12516.
39. Cardon, J. W., and Boyer, P. D. (1978) *Eur. J. Biochem. 92*, 443−448.

BI015735A